Light-scattering properties of plate and column ice crystals generated in a laboratory cold chamber

Brian Barkey, Matt Bailey, Kuo-Nan Liou, and John Hallett

Angular scattering properties of ice crystal particles generated in a laboratory cloud chamber are measured with a lightweight polar nephelometer with a diode laser beam. This cloud chamber produces distinct plate and hollow column ice crystal types for light-scattering experiments and provides a controlled test bed for comparison with results computed from theory. Ice clouds composed predominantly of plates and hollow columns generated noticeable 22° and 46° halo patterns, which are predicted from geometric ray-tracing calculations. With the measured ice crystal shape and size distribution, the angular scattering patterns computed from geometrical optics with a significant contribution by rough surfaces closely match those observed from the nephelometer.

OCIS codes: 010.1310, 010.2940, 290.5820, 290.5850.

1. Introduction

Reliable information about the single-scattering properties of nonspherical ice particles that are present in cirrus clouds is required for remote sensing applications[1] and to determine the bulk radiative properties of these clouds and their corresponding implications for the global radiation budget.[2,3] Significant progress has been made in the theoretical determination of the single-scattering properties of ice crystals of various shapes and sizes.[4,5] However, there has been little progress in the experimental determination of the scattering properties associated with ice crystal habit. Although polar nephelometers have been used on airplanes to measure ice crystal scattering properties,[6,7] it is difficult to directly compare the scattering measurements with theoretical results because of the complex and varied nature of ice crystal habits and their orientation in the direction of the incident light beam. Moreover, we also note that several nephelometers have been used in laboratory settings.[8,9] However, a rigorous laboratory examination of the scattering properties as a function of ice crystal type has not yet been accomplished to our knowledge.

The cloud chamber developed at the Desert Research Institute has been used to produce ice clouds composed of largely uniform ice crystal shapes by proper control of the temperature and humidity within the chamber. This presents a unique opportunity to study the scattering properties of ice crystals as a function of their morphology by use of a nephelometer that we have designed.[10] This lightweight nephelometer was specifically developed for use on a balloonborne platform. Thus the laboratory experiment can be used as a testing bed to verify and characterize the instrument's operation.

In this paper we first describe the polar nephelometer and cloud chamber employed in the experiment and then present two-dimensional scattering measurements when microphysical observations indicate predominantly columns and plates. These cases are chosen because, although these habits do occur in natural ice clouds, the scattering properties expected from these types are expected to be unique, hence providing an experimental demonstration of the habit dependence of scattering from ice particles. The experimental measurements are subsequently compared with theoretical expectations based on the observed crystal habit and size distribution.

2. Experimental Setup

The polar nephelometer shown in Fig. 1 has been described in more detail in our previous paper.[10] Thus only a brief description and significant changes to the instrument are described here. The instru-

B. Barkey (brian_barkey@juno.com) and K. N. Liou are with the Department of Atmospheric Sciences, University of California, Los Angeles, Los Angeles, California 90095. M. Bailey and J. Hallett are with the Desert Research Institute, Atmospheric Science Center, P.O. Box 60220, Reno, Nevada 89506.

Received 6 March 2002; revised manuscript received 2 July 2002.

0003-6935/02/275792-05$15.00/0

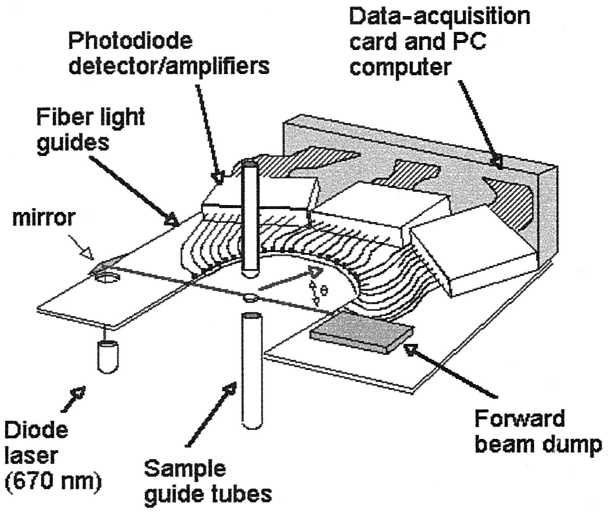

Fig. 1. Physical layout of the polar nephelometer showing how the laser beam intersects the falling ice crystals confined to the center of the fiber-optic coupled detector array by the sample tube with a 3-mm inside diameter. Not shown are the light absorbers placed above and below the scattering plane to minimize the effect of secondary internal reflections.

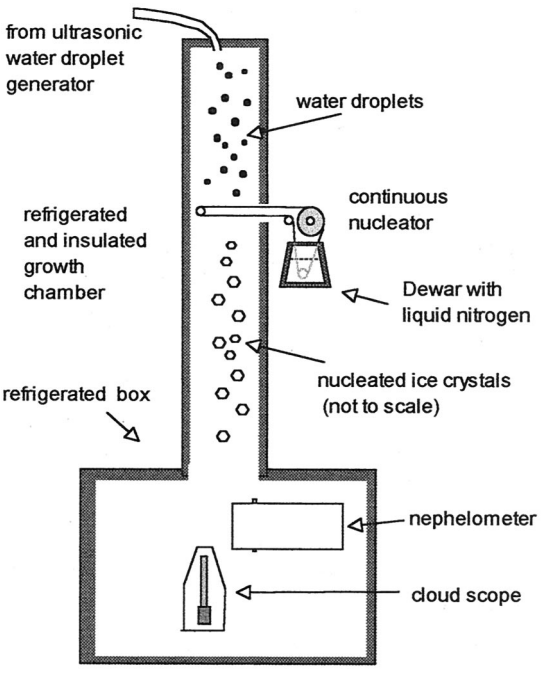

Fig. 2. Water droplets are injected into the top of the growth column and nucleated near the center. The cloud scope and polar nephelometer are placed in the cold chamber at the bottom of the growth column.

ment consists of an array of 33 discrete fiber-optic coupled photodiode detectors arranged in a two-dimensional plane to detect the scattered light intensities between the angles of 5° and 175°. A light beam highly polarized parallel to the scattering plane at a wavelength of 0.67 μm from a 35 mW laser diode is collimated into an elliptical beam, approximately 4 mm tall and 2 mm wide. This beam is then directed across the plane of detection to intercept particles that are channeled into the center of the detector array by an aluminum tube with an inside diameter of 3 mm.

The particles are removed out of the bottom of the instrument by another aluminum tube with an inside diameter of 5 mm. The gap between the sample tubes is approximately 8 mm. The laser beam exits the scattering plane into a beam absorber. Not shown in Fig. 1 are two light absorbers placed above and below the scattering plane to reduce the effect of secondary reflections within the instrument. The voltages produced by the photodiode detectors are measured by a small embedded computer and data-acquisition circuit built into the instrument, and this intensity information is then sent to another computer outside the cloud chamber for storage. The instrument has a linear response that is correct to within 1% except at the lower intensity levels, where instrument noise that produces an error of 10% defines a dynamic range of approximately 3 decades.[10] Although a single measurement of the light scattered into the array takes less than 0.05 s, operationally only approximately eight measurements per second can be transmitted to the external computer for storage.

The cloud chamber at the Desert Research Institute, shown in Fig. 2, is an upgraded unit of the chamber described in Ref. 11. It consists of an insulated and refrigerated column approximately 4 m tall and 0.3 m in diameter positioned above a larger cold chamber. Two dedicated chillers are used to control the growth column temperature above and below the nucleator, and several thermocouples are placed along the length of the growth column. Water droplets from an ultrasonic humidifier fall and cool to the desired temperature in the upper column, some of which are nucleated by a wire spring, which is continuously cooled by liquid nitrogen and presented to the ice cloud by a system of pulleys and a slowly rotating electric motor.

To some extent, the water-vapor pressure can be controlled by the rate at which water droplets are injected into the crystal chamber, but ice crystal habit is mainly controlled by the temperature at which the crystals are allowed to grow after nucleation. The nucleated ice crystals continue to grow at the expense of water droplets as they fall through the growth column and into the lower cold chamber where the polar nephelometer is placed. As the system is sealed, colder hence denser air falls to the bottom of the lower cold box, which produces a temperature stratification that retards the ice crystal free fall. Also, because of the slow fall speeds of the generated ice crystals, a suction pump is connected to the sample outlet of the polar nephelometer to pull ice crystals into the scattering volume. Simultaneously, the ice crystal microphysics are monitored by a cloud scope[11] positioned approximately 20 cm from the nephelometer sample inlet. The cloud scope is a video microscope that observes the particles

that fall onto a sapphire window. A PC-based image tool is subsequently used to analyze the recorded images.

3. Experimental and Theoretical Results

In the experiment, the volume involved in the light-scattering measurement was defined by a small cylinder 3 mm in diameter and 4 mm in length. Moreover, the ice crystal concentration measured previously in the cloud chamber[11] was normally of the order of 1 particle/2 mm^3, which corresponds to approximately 14 particles in the scattering volume. It is anticipated that the effect of multiple scattering on the nephelometer measurement can be neglected. The intensity of the light scattered into the two-dimensional plane where the fiber light guides are positioned depends on the number of particles in the scattering volume and the size, shape, and orientation of these particles. These experimental parameters vary considerably during experiments, which causes the intensity of the measured results to vary widely from one measurement to the next. The standard deviation of the measured intensity at each angle for measurements that are above the low-intensity noise level comprises 40–70% of the measured mean when determined with the results of a single cloud event of over 100 measurements. The higher variations occur at the channels associated with halo phenomena, as these intensities occur only when the crystal(s) are oriented to scatter light into the measurement plane. For these reasons, we decided to average the scattering patterns over several hundred measurements, which took approximately 2–4 min to complete. During this period it is assumed that the ice cloud habits and concentration remain constant, which is reasonable based on the cloud-scope images. It must also be assumed that the particles in the scattering volume are randomly oriented as they have smaller dimensions[12] and because the particles do not fall into the instrument, but are pulled in by a vacuum. At least 190 measurements are needed to reduce the standard error of the mean to less than 5%. In this manner, the averaged scattering pattern corresponds to an ice crystal with the scattering properties of all the particles that existed during the time period of the experiment.

Shown at the bottom of Fig. 3 is a cloud-scope video image when the crystal habit of the cloud consisted of predominantly plates and short columns grown at a temperature of approximately −6 °C. The vertical white stripe in this image is due to glare from the cloud-scope light source. Despite our use of several successive images of a single cloud event to count particles that became occluded by other falling crystals, only 50 particles are accounted for in this cloud event. The size distribution of the counted particles is shown in the histogram of Fig. 3. The particles have an average maximum dimension of 17 ± 0.5 μm and are composed of mostly plates (≈60%) and short columns. Spikes in the histogram are due to the small sample size. The average aspect ratio (or $L/2a$, where a is the radius of the hexagonal face and

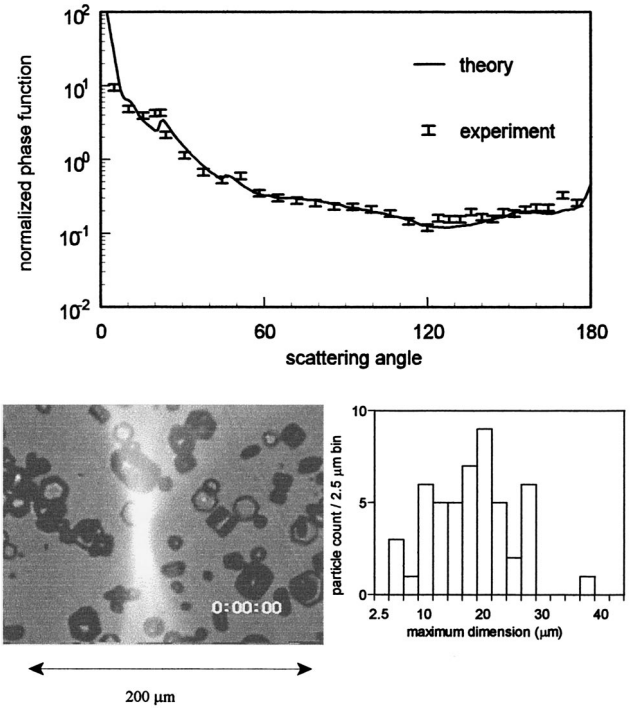

Fig. 3. Top plot is the two-dimensional angular scattering intensities measured by the polar nephelometer when predominantly plates and small columns are seen, as shown in the lower video cloud-scope image. The particle count is summarized in the histogram. The white area that can be seen in the middle of the image is due to the cloud-scope light source.

L is the length of the column or the thickness of a plate) is approximately 0.8. Because plate thickness could not be directly measured from these images, the plate thickness h is determined from $h = 0.014\, d^{0.474}$, where d is the plate diameter between 10 and 3000 μm from a parameterization in Ref. 13. Fitted to the theoretical expectation shown at the top of Fig. 3, based on the observed particle microphysics as described below, are the experimentally measured scattering properties from the average of 189 measurements taken over a period of approximately 3 min. The error bars correspond to the 5% standard error of the mean. Figure 4 is similar to Fig. 3, except that it involves a cloud event when mostly hollow columns, grown between −5 °C and −7 °C, were seen by the cloud scope. The 26 particles counted from this image consist of mostly hollow columns with an average aspect ratio of approximately 2.1 and an average maximum dimension of approximately 36 ± 0.5 μm. However, regular columns, trigonal shapes, and plates can also be seen. The experimental result is the average of 511 measurements taken over a period of approximately 4.5 min. The standard error of the mean for this result produces an approximate 3% error.

Phase functions, normalized in the manner described in Ref. 5, for simple hexagons and hollow columns calculated by geometrical-optics methods with various aspect ratios corresponding to the mea-

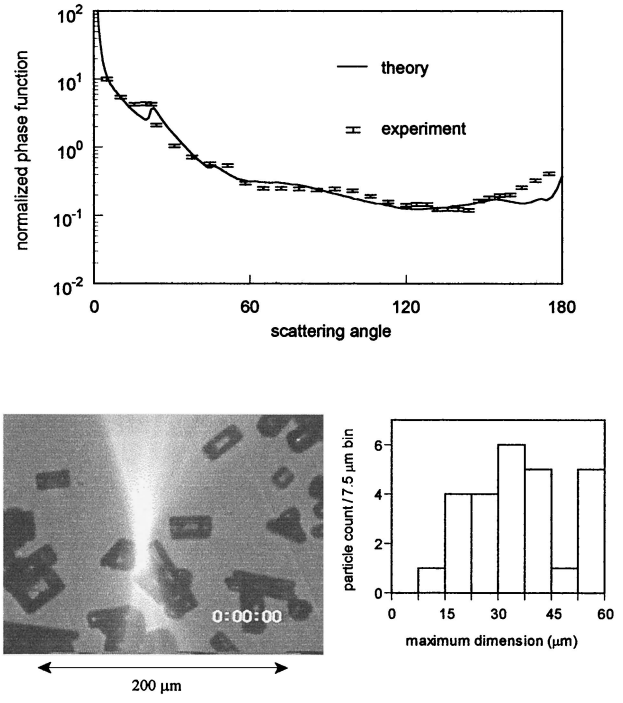

Fig. 4. Same as Fig. 3, except for a case in which columnar shapes were seen by the cloud scope.

sured crystal sizes are combined by use of the extinction cross section determined from the measured crystal size and the counted population to weight the scattering contributions of each particle. These phase functions are the combination of the Stokes parameters $P_{11} + P_{12}$ (as defined by Ref. 14), corresponding to the polarization state of the incident light and when random orientation of the particles in the scattering volume are assumed. For randomly oriented simple hexagonal particles, the extinction cross section (C_e) is approximated with[5]

$$C_e = \frac{3a^2}{2}\left[\sqrt{3} + 4\left(\frac{L}{2a}\right)\right], \tag{1}$$

where particle length L and radius a are measured directly from the images or calculated as described above. In Fig. 3, approximately 80% of the particles were assumed to have rough surfaces to account for the surface features that can be seen on some of the larger plates in the cloud-scope image. Substantial surface roughness (as defined in Ref. 4) was incorporated in the phase functions by random perturbations of the crystal surface.[4,15] In Fig. 4 approximately 10% of the phase functions used to produce the theoretical values are based on the hollow column habit. The other particles are simple columns and plates, of which 80% have rough surfaces.

Overall, the experimental results closely follow the theoretical values. Both the 22° and 46° halo intensity imprints are clearly displayed, although there is less intensity at the 46° feature for the hollow column case. This is expected as the 46° halo feature is produced by refraction through a 90° prism, which is more prevalent in plates than in columns. For both results, a large percentage of the theoretical expectations required particles with rough surfaces to provide a reasonable fit to the experimental results. This is most likely due to surface features on the particles that cannot be seen on the cloud-scope images because of the low resolution of the video camera or smaller particles not seen by the cloud scope. Smaller particles have lower collection efficiencies. For particles collected by use of gravitational sedimentation, a cutoff at 7 μm has been estimated for an automated replicator system previously used in this chamber.[11] Despite use of a large percentage of particles with rough surfaces in the expectation, there is still more measured light scattered into the angles between 10° and 20° than expected.

Note that the expectation did not include several particle habits, including the trigonals mentioned above, the end features that can be seen on some of the columns of Fig. 4, and the particles that are too small or too irregular to classify as can be seen in Fig. 3. The measured intensity between 160° and 175° of Fig. 4 is much higher than expected, which is most likely caused by these limitations in the determination of the microphysical properties. Between 120° and 160°, the experimental result is not smooth in both cases, which is due to systematic errors in the calibration that are more noticeable at lower intensities. There is a slight difference between the angular position of both the 22° and the 46° intensity peaks because each fiber optic senses light scattered into an angle of approximately 2°, and the angular positions of the fiber optics are not at the points of maximum scattered intensity.

4. Summary

A new lightweight polar nephelometer is used to study the light scattered by ice crystals into a two-dimensional plane by two different and distinct cloud types: a cloud composed of plates and one composed of primarily hollow columns. The microphysical properties of the cloud as determined by concurrent video microscope images are used to develop phase function expectations derived from geometrical optics methods. Within the degree to which it is possible to determine the microphysical properties of the ice cloud, the expectation matches the experimental method.

The presence of both the 22° and the 46° intensity features, which are caused by refraction through the 60° and 90° prisms of the ice crystals, is seen in the experimental results, and it is noted that the 46° feature is more prominent for the plate cloud, as is expected. To match the experimental result, a large percentage of the particles used in the expectation have rough surfaces, which could be due to either surface features on the particles that are not visible on the cloud scope or the presence of small particles that were not captured by the cloud scope. There is some evidence of micrometer-sized roughness on ice surfaces,[16] but this is by no means comprehensive. It is also noted that other polar nephelometer

measurements[6–8] of ice particle scattering also exhibit the same features, i.e., little or no halo phenomena and smooth scattering profiles.

The authors are grateful to Y. Takano for assistance in the theoretical interpretations presented in this paper and the two anonymous reviewers for their insightful comments. This research was supported by National Science Foundation grant ATM-99-07924 and U.S. Air Force Office of Scientific Research grant F49620-01-1-0057.

References

1. P. Rolland, K. N. Liou, M. D. King, S. C. Tsay, and G. M. McFarquhar, "Remote sensing of optical and microphysical properties of cirrus clouds using Moderate-Resolution Imaging Spectroradiometer channels: methodology and sensitivity to physical assumptions," J. Geophys. Res. **105,** 11721–11738 (2000).
2. K. N. Liou, "Influence of cirrus clouds on weather and climate processes: a global perspective," Mon. Weather Rev. **114,** 1167–1199 (1986).
3. K. N. Liou, *Radiation and Cloud Processes in the Atmosphere: Theory, Observation and Modeling* (Oxford U. Press, Oxford, UK, 1992).
4. P. Yang and K. N. Liou, "Single-scattering properties of complex ice crystals in terrestrial atmosphere," Contrib. Atmos. Phys. **71,** 223–248 (1998).
5. Y. Takano and K. N. Liou, "Solar radiative transfer in cirrus clouds. I: Single-scattering and optical properties of hexagonal ice crystals," J. Atmos. Sci. **46,** 3–19 (1989).
6. S. Oshchepkov, H. Isaka, J. F. Gayet, A. Sinyuk, F. Auriol, and S. Havemann, "Microphysical properties of mixed-phase and ice clouds retrieved from in situ airborne 'polar nephelometer' measurements," Geophys. Res. Lett. **27,** 209–212 (2000).
7. R. P. Lawson, A. J. Heymsfield, S. M. Aulenbach, and T. L. Jensen, "Shapes, sizes and light scattering properties of ice crystals in cirrus and a persistent contrail during SUCCESS," Geophys. Res. Lett. **25,** 1331–1334 (1998).
8. K. Sassen and K. N. Liou, "Scattering of polarized laser light by water droplet, mixed-phase and ice crystal clouds. Part I: Angular scattering patterns," J. Atmos. Sci. **36,** 838–851 (1979).
9. A. Pluchino, "Scattering photometer for measuring single ice crystals and evaporation and condensation rates of liquid droplets," J. Opt. Soc. Am. A **4,** 614–620 (1987).
10. B. Barkey and K. N. Liou, "Polar nephelometer for light-scattering measurements of ice crystals," Opt. Lett. **26,** 232–234 (2001).
11. W. P. Arnott, Ya Y. Dong, and J. Hallett, "Extinction efficiency in the infrared (2–18 mm) of laboratory ice clouds: observations of scattering minima in the Christiansen bands of ice," Appl. Opt. **34,** 541–551 (1995).
12. J. D. Klett, "Orientation model for particles in turbulence," J. Atmos. Sci. **52,** 2276–2285 (1995).
13. H. R. Pruppacher and J. D. Klett, *Microphysics of Clouds and Radiation* (Reidel, Dordrecht, The Netherlands, 1980), p. 40.
14. H. C. van de Hulst, *Light Scattering by Small Particles* (Dover, New York, 1957), Chap. 5.
15. P. Yang and K. N. Liou, "A geometric-optics integral-equation method for light scattering by nonspherical ice crystals," Appl. Opt. **35,** 6568–6584 (1996).
16. J. D. Cross, "Study of the surface of ice with a scanning electron microscope," in *Physics of Ice: Proceedings of the International Symposium on Physics of Ice*, N. Riehl, B. Bullemer, and H. Engelhardt, eds. (Plenum, New York, 1969), pp. 81–94.